ELSEVIER

Journal of Alloys and Compounds 458 (2008) 231–237

Journal of ALLOYS AND COMPOUNDS

www.elsevier.com/locate/jallcom

Age-induced four-stage transformation in Ni-rich NiTi shape memory alloys

L.J. Chiang [a], C.H. Li [a], Y.F. Hsu [b], W.H. Wang [a,*]

[a] *Department of Materials Science and Engineering, National Taiwan University, No. 1, Sec. 4, Roosevelt Road, Taipei 106, Taiwan, ROC*
[b] *Department of Materials and Mineral Resources Engineering, National Taipei University of Technology, Taipei 106, Taiwan, ROC*

Received 19 March 2007; received in revised form 30 March 2007; accepted 2 April 2007
Available online 6 April 2007

Abstract

A four-stage transformation has been observed in an aged Ti–50.7 at.%Ni shape memory alloy by differential scanning calorimetry (DSC). Such phenomenon is able to occur in the alloys with compositions around 50.7 at.%Ni by aging at 673 K. The multi-stage transformation behavior observed in this study is attributed to the complex microstructural evolution, i.e., formation of large-scale and small-scale heterogeneities which induced various stress fields and affected the phase transformation sequence.

Keywords: Precipitation; Grain boundaries; Thermal analysis

1. Introduction

It is well known that NiTi alloys are considered to be the most important shape memory alloys by exhibiting excellent shape memory effect, superelasticity and good mechanical properties [1–3]. After certain thermomechanical treatments or adding a third element [1–4], the transformation sequence can be changed from one-stage (B2-M) to two-stage (B2-R, R-M) transformation on cooling. The three kinds of B2-R, R-M and B2-M transformations can be characterized by different features of temperatures hysteresis and transformation energy [5–7].

In recent years, Ni-rich NiTi alloys were discovered to exhibit more complex three-stage martensitic transformation (multiple-stage transformation; MST) after aging between 573 and 773 K for appropriate time [5,8–16]. Morawiec et al. [8–10] suggested a scenario associated with heterogeneous arrangement of dislocations for a solution-treated NiTi material followed by cold-deforming and subsequent aging. Another explanation invoking coherent stress field around Ni_4Ti_3 precipitates to rationalize this three-stage transformation is suggested by Bataillard et al. [11]. By in situ TEM study, they proposed that the coherent stress field around precipitates during aging favors the nucleation of both R phase and B19′ martensite. Therefore, the first two transformations occur in regions affected by coherent stress field and the last transformation occurs in regions away from coherent stress field. In 2002, Khalil-Allafi et al. [12] proposed a mechanism based on: (1) the local composition inhomogeneity between precipitates and (2) different nucleation barriers for R phase (small) and B19′ martensite (large). Obviously, all these explanations were proposed on the basis of "small-scale heterogeneity". Recently, Fan et al. [6] performed aging treatments of two binary single crystals and two corresponding artificial polycrystals to demonstrate a "large-scale heterogeneity" of grain boundary precipitation on multiple-stage transformation and therefore the possibility of small-scale heterogeneity such as local stress field can be excluded. However, Michutta et al. [15] provide another evidence to support the effect of small-scale heterogeneity in single crystal for aging in higher temperature.

In addition, under some thermomechanical treatments, a four-stage transformation has been reported from annealing of materials subjected to cold-working without being solution-treated. The explanations and microstructures associated with non-homogeneous distribution of dislocations [17] or of grain size [18] were proposed and documented to result in two B2-R and two R-M transformations.

So far it is concluded that the multiple-stage transformation can be attributed to: (1) small-scale heterogeneity (local difference in stress field and composition between precipitates) from

* Corresponding author. Tel.: +886 233662739; fax: +886 223634562.
E-mail address: whwang@ntu.edu.tw (W.H. Wang).

0925-8388/$ – see front matter © 2007 Elsevier B.V. All rights reserved.
doi:10.1016/j.jallcom.2007.04.006

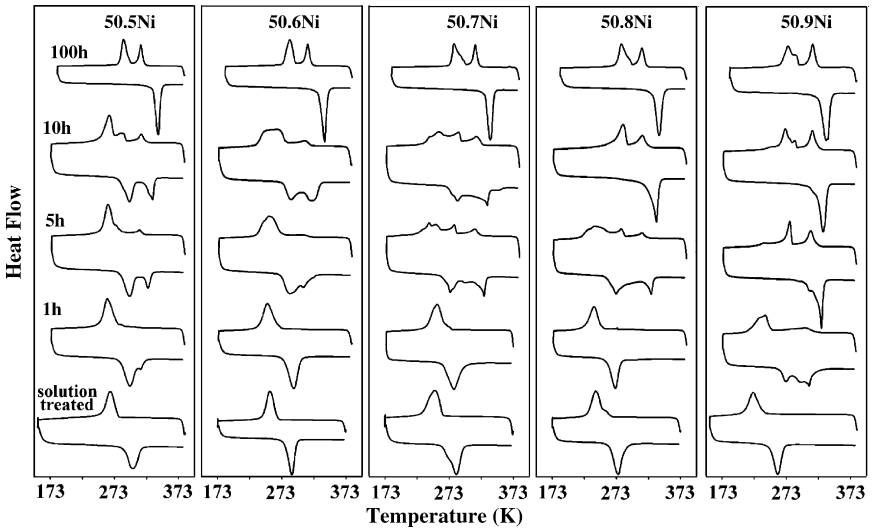

Fig. 1. DSC curves for 50.5–50.9 at.%Ni materials after solution-treated and aged at 673 K for 1, 5, 10 and 100 h, respectively.

uniform precipitation in materials or (2) large-scale heterogeneity resulting from grain boundary precipitation and an almost precipitate-free grain interior or (3) effects of thermomechanical process. The main object of this study is to perform a new four-stage transformation caused only by aging without other thermomechanical treatments and to provide a new microstructural explanation combining large and small heterogeneities. In this paper, both the large-scale heterogeneity (grain boundary precipitation) and small-scale heterogeneity (local stress field) are considered to be responsible for the aging-induced four-stage transformation.

2. Experimental procedures

Five binary Ni-rich NiTi shape memory alloys, with 50.5–50.9 at.% of Ni, were prepared by a conventional tungsten arc-melting technique (VAR). All the ingots were hot-rolled at 1173 K into thin plates and then cut into test specimens. In hot rolling procedures, the rolling direction of the ingots was rotated 90° in the next rolling pass to decrease the effects of texture. Specimens (10 mm × 10 mm × 1 mm) were sealed into quartz tubes and solution-treated at 1173 K for 1 h then followed by quenching into water. After solution treating, aging treatments were carried out at 673 K for various periods of time (5–100 h).

Transformation behaviors and characteristic temperatures of specimens were studied using a DSC-910 differential scanning calorimeter (DSC) with a constant cooling and heating rate of 10 K/min. The method of partial DSC cycles was employed to investigate the sequences of multi-stage transformation. Measurement of the Vickers microhardness was taken by a Future-tech microhardness tester. SEM micrographs were taken by using a LEO-1530 field emission scanning electron microscope. TEM examination was also performed by using a JEOL-2000EX transmission electron microscope operating at 200 kV. Specimens for TEM examinations were prepared by a double jet thinning technique using an electrolyte of 20% sulfuric acid and 80% methyl alcohol operating at 273–278 K.

3. Results and discussion

3.1. DSC results

The DSC curves of the five Ni-rich NiTi alloys aged at 673 K for various periods of time are shown in Fig. 1. It is clearly seen that, after solution treatment, all the materials with different Ni content undergo one-stage B2-B19′ martensitic transformation with a temperature hysteresis about 35 K. When the well solution-treated materials are subjected to age at 673 K, a systematic evolution with aging time can be observed on cooling. The multiple-stage transformation occur in the aged specimens for 5 and 10 h, and then change into a two-stage transformation behavior with increasing aging time to 100 h. Moreover, it is important to highlight that the four-stage transformation can be observed in 50.7 at.%Ni alloy aged for 5 and 10 h, and in 50.8 at.%Ni alloy aged for 5 h. This implies that, under 673 K aging treatment, the aging-induced four-stage transformation behaviors can occur in a narrow range of composition from 50.7 to 50.8 at.%Ni.

In order to investigate the nature of the four transformation peaks, the technique of partial DSC cycles was employed on the 50.7 at.%Ni sample aged at 673 K for 5 h, as shown in Fig. 2. Four pairs of transformation peaks (the peak on cooling and its corresponding peak on heating; peak 1–1′, peak 2–2′, peak 3–3′, peak 4–4′,) were observed and characterized respectively by their temperature hysteresis of 7, 46, 36 and 38 K. The results suggest that the first pair of transformation of peak 1–1′ should be the B2-R transformation owing to its small temperature hysteresis of 7 K. In contrast, the other three pairs of transformations can be attributed to martensitic transformations as their large temperature hysteresis. However, the second pair of transformation peaks has a larger temperature hysteresis of 46 K than the last two and should be expected for R-M transformations due to the fact that $|\Delta S^{\text{R-M}}| < |\Delta S^{\text{B2-M}}|$ [5]. Moreover, the reverse curve of this second partial DSC cycle does not exhibit any small temperature hysteresis which implies that the R phase had fully transformed into B19′ martensite so that no small temperature hysteresis was observed in the reverse curve. Subsequently, the last two pairs of transformations can be referred to B2-M transformation as the temperature hysteresis is about 35 K which is a typical characteristic of martensitic transformation and is consistent to those observed in solution-treated materials. It is concluded that the

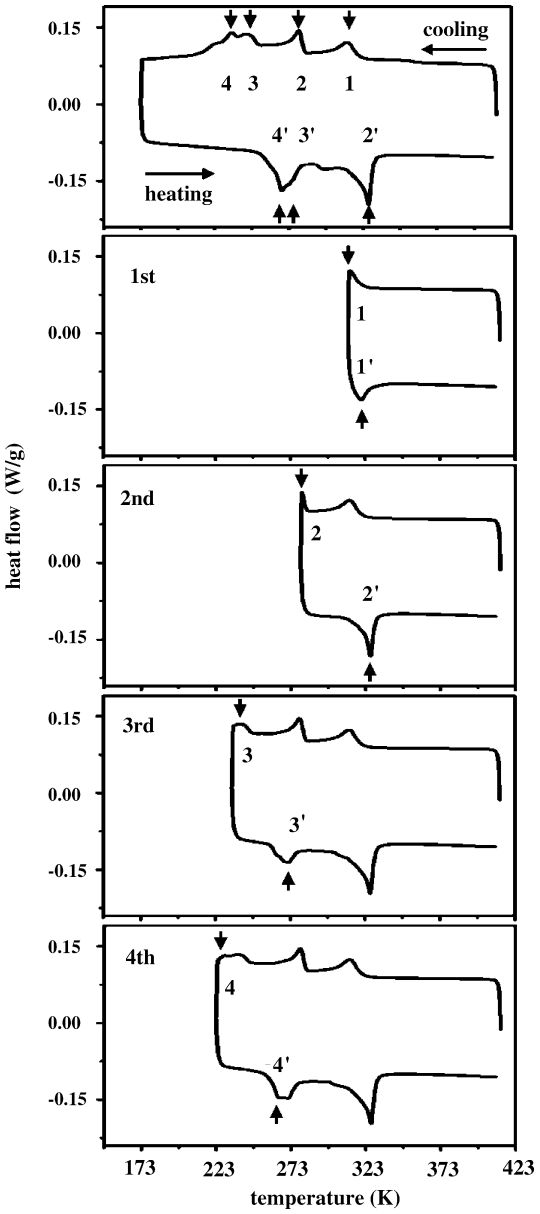

Fig. 2. Partial DSC cycles and full cycle for 50.7 at.%Ni aged at 673 K for 5 h.

50.7Ni material aged at 673 K for 5 h exhibits a four-stage transformation behavior containing one B2-R transformation, one R-M transformation and two B2-M transformations on cooling (denoted as R-M_1-M_2-M_3) sequentially.

3.2. Optical microstructure and hardness

Fig. 3(a) shows the optical micrograph obtained from the cross-section of the solution-treated 50.7Ni alloy, in which a microstructure with homogeneous grain size of about 80 μm and uniform shape is observed. It was evident that there is little texture presented after hot rolling and subsequent solution treatment. Fig. 3(b) shows the distribution of Vickers microhardness of the whole cross-section. There are no significant differences in hardness from specimen surfaces to the central part. This implies strain recovery and recrystallization were accomplished

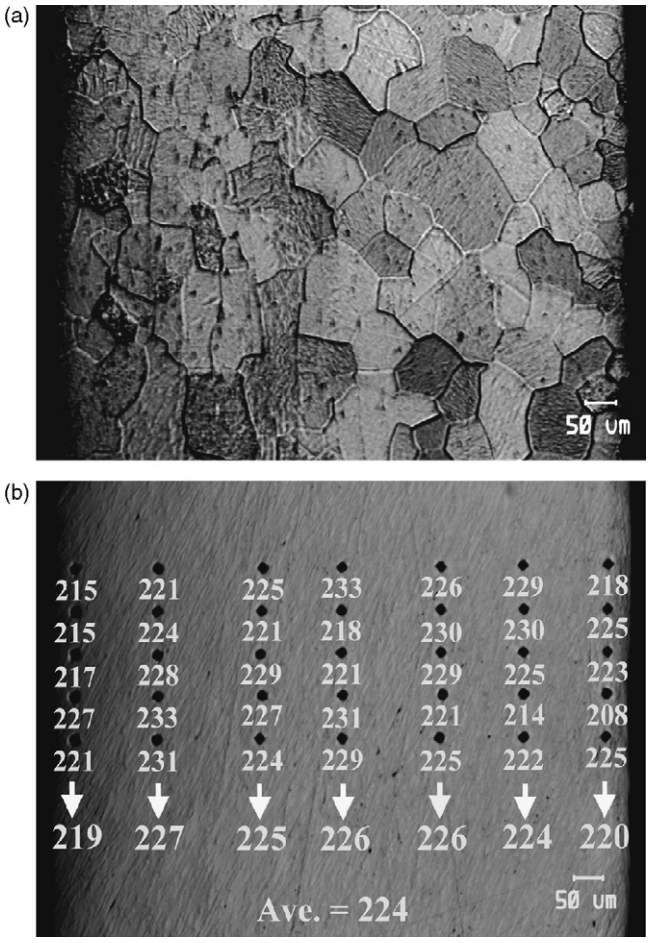

Fig. 3. (a) A cross-sectional morphology showing homogeneous grain size of solution-treated 50.7 at.%Ni alloy. (b) The corresponding hardness (Vickers) of the cross-section area.

by solution treatment at 1173 K for 1 h. Moreover, it suggests that there is no inhomogeneous distribution of internal stresses remaining in the well solution-treated material.

3.3. Effects of aging on hardness and Ni_4Ti_3 precipitation

A hardness examination was made to evaluate the variations of coherent stress field resulting from Ni_4Ti_3 precipitates. As shown in Fig. 4, an obvious precipitation hardening behavior was revealed in the 50.7Ni alloy aged at 673 K for various aging time. The hardness for 5 h aging reached the highest value. With increasing aging time the hardness decreased from the highest value in 5 h through 10 h to the lowest value in 100 h. The result indicates that a strongest coherent stress field arose when the specimen was aged for 5 h so that it can be related to the existence of the coherent Ni_4Ti_3 precipitates. When the aging time is longer than 5 h, the Ni_4Ti_3 precipitates gradually lost their coherency and the associating hardness decreased. It also ought to be pointed out that, as the hardness changed with aging time, the phases present at room temperature also changed, since the transformation temperatures of R phase and B19′ martensite are varied with aging time.

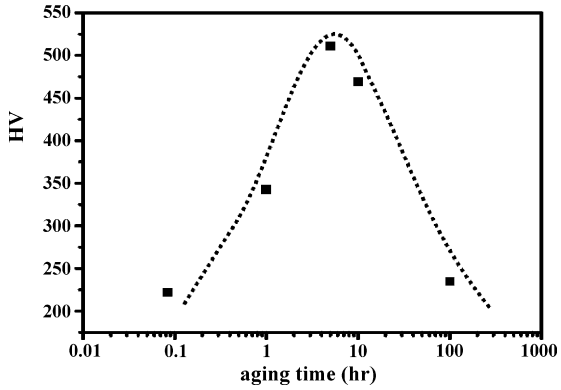

Fig. 4. Variation of Vickers hardness of 50.7Ni alloy during aging at 673 K.

Fig. 5 shows the SEM micrographs of specimens aged for 5 and 100 h. It was evident that two kinds of heterogeneous distribution of Ni_4Ti_3 particles were observed on the grain boundary and in grain interior. Firstly, precipitation of small Ni_4Ti_3 particles with a lenticular shape congregated along the grain boundaries. The density of Ni_4Ti_3 precipitates is largest in the grain boundary region. Secondly, the distribution of Ni_4Ti_3 precipitates in grain interior is also not uniform and can be distinguished into higher (area A) and lower (area B) precipitate

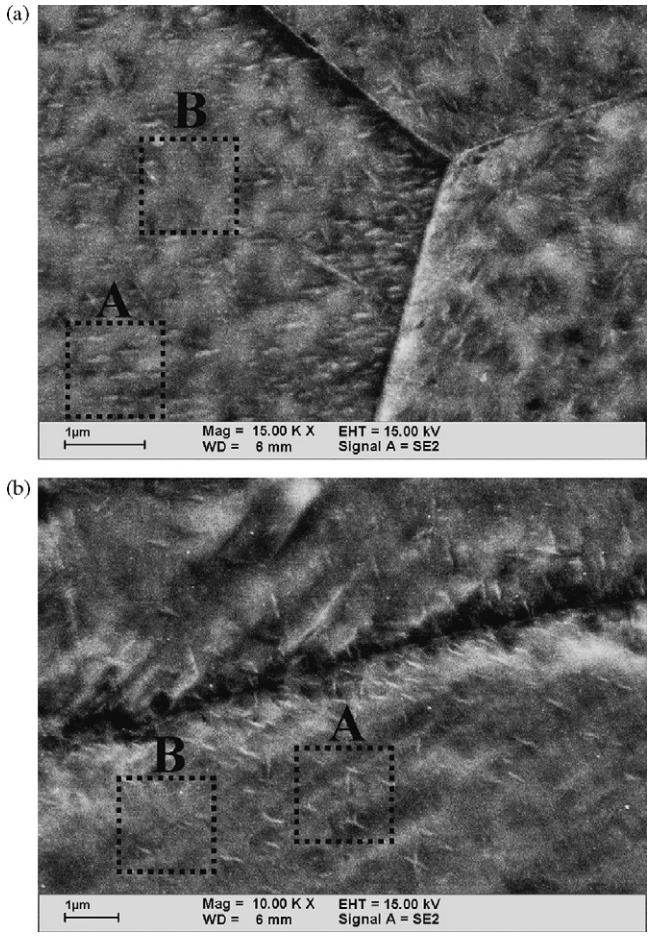

Fig. 5. SEM micrographs showing the heterogeneous precipitation of 50.7 at.%Ni alloy aged for: (a) 5 h and (b) 100 h.

density regions. Also the interspacing between precipitates is not the same as shown in Fig. 5. However, there is no significant difference in particle size between the two aging conditions.

3.4. TEM observations

3.4.1. Regions along grain boundaries

TEM examinations were performed on the selected 50.7Ni sample that was aged for 5 h and exhibited a four-stage transformation. The conditions for thin foil specimen preparation (273–278 K) and TEM observation (298 K) were similar to the second partial DSC cycle as shown in Fig. 2. Therefore, the specimen had already experienced one B2-R and one R-M transformation. In such conditions, two different microstructures were found in the grain boundary region and grain interior. As shown in Fig. 6, a heterogeneous martensitic transformation in the grain boundary region (~2.5 μm in width) is documented and proven by the corresponding SAD pattern of B19′ martensite along [2 0 1] zone-axis. However, the grain interior still remained in B2 phase and was also recognized by its corresponding SADP of B2 [1 1 1] zone-axis.

Fig. 6 provides a direct evidence for where the first two transformations occurred and prove exactly what these phases are by the SAD patterns. Consequently, the first distinct DSC peak on cooling is attributed to the transformation from B2 to R phase in the regions near grain boundary with congregated Ni_4Ti_3 precipitates. And this is because the congregated Ni_4Ti_3 precipitates provide strongest stress field to encourage the nucleation of R phase. When further cooling to the temperature for jet polishing (273–278 K) the previous R phase in regions of grain boundary transformed into B19′ phase. Therefore, the heterogeneous martensitic transformations near grain boundaries are clearly visible. This illustrates how the "large-scale heterogeneity" of grain boundary precipitations can affect and induce multi-stage transformation.

3.4.2. Grain interior

The TEM observations unambiguously show that the first two distinct DSC peaks are associated with B2-R and R-M transformations occurring in the grain boundary region with congregated Ni_4Ti_3 precipitates. Consequently, the last two transformations can be related to occur in grain interior. In Fig. 7 it is confirmed that some B2 matrix around Ni_4Ti_3 precipitates have transformed into R phase. The morphology of R phase nucleated around Ni_4Ti_3 precipitates (Fig. 7(a)) is documented and identified by the SAD pattern with 1/3 R phase extra points and 1/7 Ni_4Ti_3 extra points of a beam direction parallel to B2 [1 1 2] zone-axis as well as parallel to R phase [−2 1 2] and Ni_4Ti_3 [1 1 0] zone-axis as shown in Fig. 7(b). In Fig. 8(a), the presence of growing B19′ martensite was also discovered to form with a long and sharp B2/B19′ interface along one specific direction. A further zoomed-out micrograph of a small initial-growing one, as circled by white dotted line, and its corresponding SAD pattern provide a direct evidence of B19′ martensite nucleating between two Ni_4Ti_3 precipitates as shown in Fig. 8(b and c). It tends to suggest that the formation of B19′ martensite was triggered due to the strong coherent stress field from two adjacent

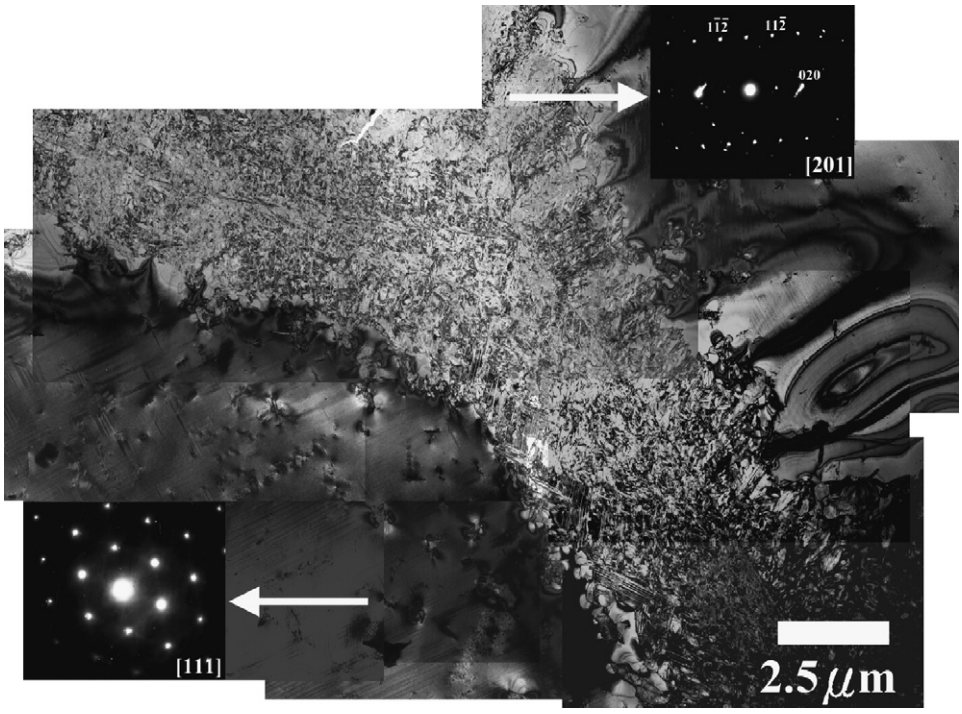

Fig. 6. TEM bright field image of 50.7Ni alloy aged for 5 h showing two different microstructures and corresponding SADPs near and away from grain boundaries.

precipitates. Furthermore, Tirry and Schryvers [19,20] pointed out that the compressive strain field is in front of every precipitate and the expansive strain is at the interface. Therefore, all these precipitate-induced local stress fields can be expected to be oriented and connected due to the arrangement of Ni_4Ti_3 precipitates in matrix that are oriented, too. This is why the growing B19′ martensite induced by oriented stress field to grow in preferential directions. Fig. 8(a) shows this kind of growth that is characterized by the B2/B19′ interfaces moving toward matrix in preferential directions. The positions indicated by arrows present evidence of discontinuous growing and imply the growing of B19′ martensite is bound for and connected by the adjacent precipitates and their oriented local stress field. Therefore, the third transformation peak on cooling could be attributed to the local oriented and connected stress field which favors the B19′ martensite to grow in preferential directions. This is considered to occur in the areas of high precipitate density as shown in Fig. 7(a), as the interspacing between precipitates is similar and smaller that the oriented stress field can be expected to be dominant.

As for the fourth transformation peak on cooling, it may be consequently attributed to the expansion of B19′ martensite and consuming of untransformed B2 phase with movement of the B2/B19′ interfaces into matrix. Finally, all the transformations in grain interior could be suggested as the results of "small-scale heterogeneity" in local stress field.

3.5. Origin of four-stage MST

According to these results, the origin of four-stage transformation (R-M_1-M_2-M_3) observed in this study is suggested by comparing with other experimental results and mechanisms reported in the previous literatures [5–18]. The 50.7Ni alloy used in this study was hot-rolled and then solution-treated. Its microstructure reveals a uniform grain size and fully annealed status as shown in Fig. 3 so that the effect causing four-stage transformation such as difference in grain size [18] and heterogeneous arrangement of dislocations [17] cannot apply to the present study.

Moreover, being different from homogeneous precipitation, the mechanism of local stress field between precipitates suggested by Khalil-Allafi et al. [12,13] and Bataillard et al. [11] cannot fully account for this study. Furthermore, since the precipitation of Ni_4Ti_3 is able to occur in both grain boundaries and grain interiors in this study, another explanation [14] designed from the microstructures of a grain boundary precipitation and an almost precipitates-free grain interior also cannot apply well in the present work.

Now we consider the effect of large-scale heterogeneity in chemical composition between grain boundary and grain interior. In our study, the heterogeneous precipitations in grain boundaries and grain interiors both occurred in short (5 h) and long (100 h) aging time, as shown in Fig. 4. Therefore, the heterogeneity in composition between grain boundary and grain interior should be remaining in both 5 and 100 h samples. However, the multiple-stage transformation behavior merely can be observed in sample aged for 5 h but not in the one of 100 h, as shown in Fig. 1. This implies that the large-scale heterogeneity in chemical composition between grain boundary and grain interior does not dominate the multiple-stage transformation behavior in the present study. Nevertheless, compared to the result with the precipitation hardening curve shown in Fig. 4, it is clear that the variation of hardness with aging time can match the evolution of four-stage transformation. It suggests a highly pos-

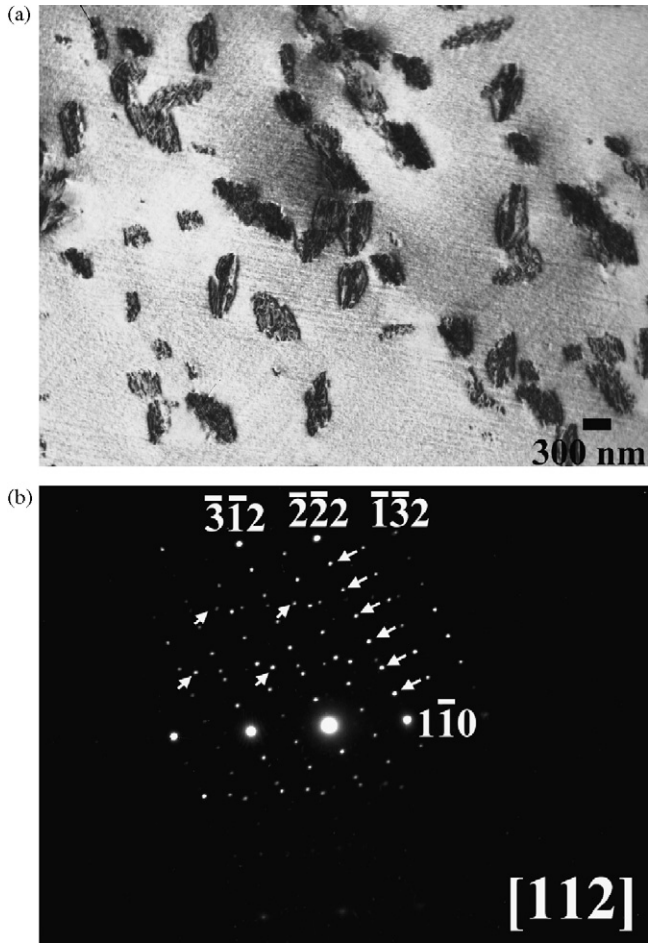

Fig. 7. TEM micrographs taken from grain interior of the 50.7Ni alloy aged for 5 h showing: (a) R phase nucleated around the Ni_4Ti_3 precipitates and (b) the corresponding SAD pattern of B2 [1 1 2] zone-axis showing 1/3 R phase and 1/7 Ni_4Ti_3 extra points.

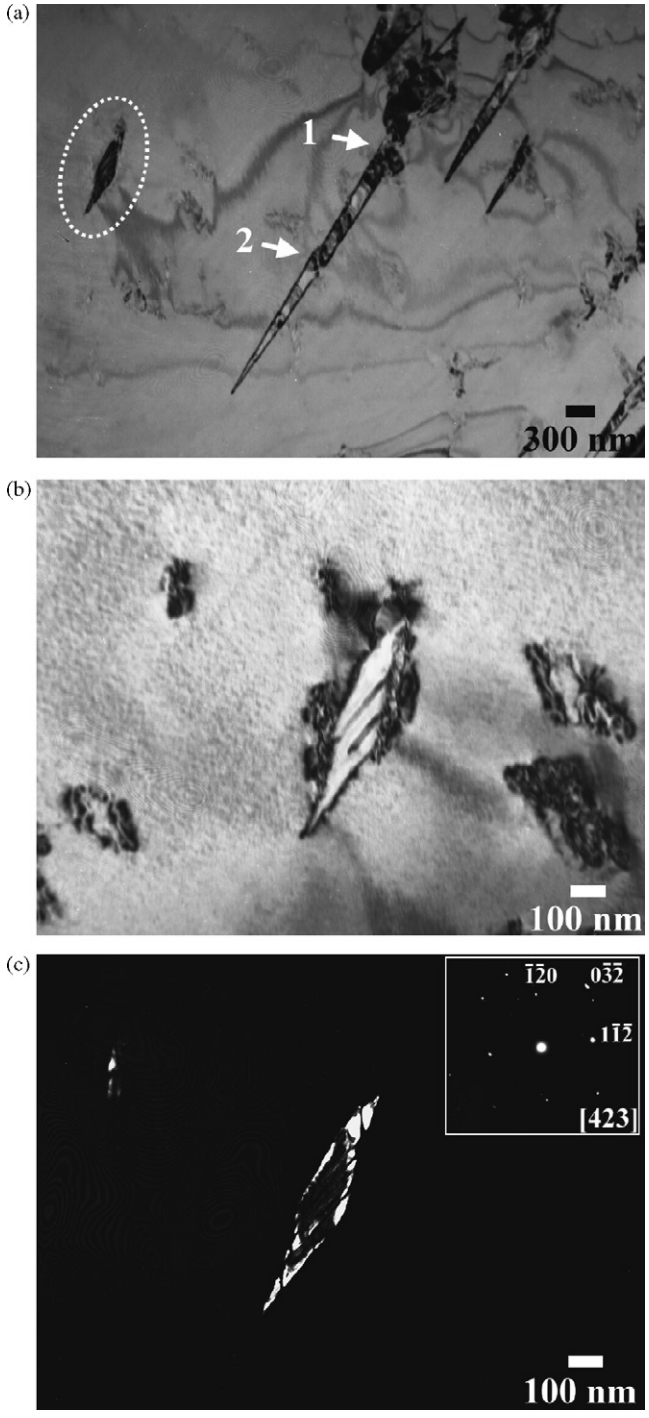

Fig. 8. (a) The growing B19′ martensite with long and sharp interfaces, (b) the nucleation of B19′ martensite highlighted in (a) and (c) the corresponding dark field image.

sible scenario that the four-stage transformation could be related to the coherent stress field resulting from Ni_4Ti_3 precipitates. The heterogeneous distributions of Ni_4Ti_3 precipitates in grain boundary and in grain interior lead to a heterogeneous arrangement of coherent stress field in materials. Unambiguously, the regions near grain boundary suffer the strongest stress field due to the congregated Ni_4Ti_3 precipitates and form a large-scale heterogeneity in coherent stress field. For the same reason, the heterogeneous distributions of Ni_4Ti_3 precipitates in grain interior also induced a heterogeneous distribution of stress field and formed a small-scale heterogeneity in local coherent stress field. Therefore, it is considered that both the large-scale and small-scale heterogeneity in coherent stress field should be responsible for the four-stage transformation in the present study.

It also can be expected that the large-scale heterogeneity of grain boundary precipitation will dominate if we increase aging temperature to result in a large diffusion distance of Ni. On the contrary, the small-scale heterogeneity with local stress field will dominate when the aging temperature is decreased. In this paper, an effort was made to provide an explanation for an age-induced four-stage transformation by combining both large-scale and small-scale heterogeneities. Further work of in situ observation is required to investigate the behaviors of reverse transformation.

4. Conclusions

In summary, an age-induced four-stage transformation was discovered to occur in a narrow range of composition from 50.7 at.%Ni to 50.8 at.%Ni for aging at 673 K. The transforma-

tion sequence on cooling was identified to be B2-R, R-M, B2-M and B2-M sequentially. The first two transformations on cooling were suggested to occur in the regions along grain boundary while the last two were suggested to occur in grain interior. The origin of the four-stage transformation was proposed to be the heterogeneous precipitation both in grain boundary and in grain interior. The heterogeneous precipitations result in the formation of large-scale and small-scale heterogeneities which induce various stress fields and affect the phase transformation sequence.

Acknowledgement

The authors gratefully acknowledge the financial support for this research from the National Science Council (NSC), Taiwan, Republic of China, under Grant No. NSC94-2216-E002-017.

References

[1] K. Otsuka, X. Ren, Prog. Mater. Sci. 50 (2005) 511–678.
[2] H. Funakubo, Shape Memory Alloys, Gordon and Breach Science Publishers, OPA, Amsterdam, 1987.
[3] K. Otsuka, C.M. Wayman, Shape Memory Materials, Cambridge University Press, Cambridge, 1998.
[4] H. Hosoda, S. Hanada, K. Inoue, T. Fukui, Y. Mishima, T. Suzuki, Intermetallics 6 (1998) 291–301.
[5] J.I. Kim, Y. Liu, S. Miyazaki, Acta Mater. 52 (2004) 487–499.
[6] G. Fan, W. Chen, S. Yang, J. Zhu, X. Ren, K. Otsuka, Acta Mater. 52 (2004) 4351–4362.
[7] Y. Zhou, J. Zhang, G. Fan, X. Ding, F. Sun, X. Ren, K. Otsuka, Acta Mater. 53 (2005) 5365–5377.
[8] H. Morawiec, D. Stroz, D. Chrobak, Phys IV C2 (1995) 205–209.
[9] H. Morawiec, D. Stroz, T. Goryczka, D. Chrobak, Scr. Mater. 35 (1996) 485–490.
[10] D. Chrobak, D. Stroz, H. Morawiec, Scr. Mater. 48 (2003) 571–576.
[11] L. Bataillard, J.-E. Bidaux, R. Gotthardt, Philos. Mag. 78 (1998) 327–344.
[12] J. Khalil-Allafi, X. Ren, G. Eggeler, Acta Mater. 50 (2002) 793–803.
[13] J. Khalil-Allafi, A. Dlouhy, G. Eggeler, Acta Mater. 50 (2002) 4255–4274.
[14] A. Dlouhy, J. Khalil-Allafi, G. Eggeler, Philos. Mag. 83 (2003) 339–363.
[15] J. Michutta, Ch. Somsen, A. Yawny, A. Dlouhy, G. Eggeler, Acta Mater. 54 (2006) 3525–3542.
[16] Y. Liu, H. Yang, A. Voigt, Mater. Sci. Eng. A 360 (2003) 350–355.
[17] D. Chrobak, D. Stroz, Scr. Mater. 52 (2005) 757–760.
[18] S.H. Chang, S.K. Wu, G.H. Chang, Scr. Mater. 52 (2005) 1341–1346.
[19] W. Tirry, D. Schryvers, Mater. Sci. Eng. A 378 (2004) 157–160.
[20] W. Tirry, D. Schryvers, Acta Mater. 53 (2005) 1041–1049.